

Electronic relaxation dynamics of carbon cluster anions: Excitation of the $\tilde{C}^2\Pi_g \leftarrow \tilde{X}^2\Pi_u$ transition in C_6^-

Christian Frischkorn,^{a)} Arthur E. Bragg, Alison V. Davis, Roland Wester, and Daniel M. Neumark

Department of Chemistry, University of California, Berkeley, California 94720 and Chemical Sciences Division, Lawrence Berkeley National Laboratory, Berkeley, California 94720

(Received 16 August 2001; accepted 4 October 2001)

Anion femtosecond photoelectron spectroscopy (FPES) has been used to monitor intramolecular electronic relaxation dynamics following the excitation of the $\tilde{C}^2\Pi_g \leftarrow \tilde{X}^2\Pi_u$ 0_0^0 electronic transition in C_6^- . The time-dependent photoelectron spectra provide a detailed picture of the relaxation dynamics in which the initially excited $\tilde{C}^2\Pi_g$ ($v=0$) level evolves into highly vibrationally excited C_6^- in its ground electronic state. The spectra show evidence for a two-step relaxation mechanism: internal conversion (IC) to vibrationally excited $\tilde{B}^2\Sigma_u^+$ and $\tilde{A}^2\Sigma_g^+$ states, occurring on a time scale of 730 ± 50 fs, followed by IC from these intermediate states to highly vibrationally excited levels in the $\tilde{X}^2\Pi_u$ ground state with a time constant of 3.0 ± 0.1 ps. © 2001 American Institute of Physics. [DOI: 10.1063/1.1421378]

I. INTRODUCTION

For many decades, pure carbon molecules have attracted much attention due to their importance in astrophysics, chemistry, and materials science. They are believed to be components of celestial bodies, including carbon stars, comets, and molecular clouds, and have been proposed as carriers of the diffuse interstellar bands (DIB's).^{1,2} Small carbon clusters have been proposed to play vital roles in chemically significant processes such as combustion, soot formation, the chemical vapor deposition of diamonds,³ and the formation of fullerenes⁴ and carbon nanotubes.⁵ These findings and possible applications have stimulated fundamental experimental and theoretical work on the spectroscopy and dynamics of carbon clusters, much of which has been summarized in two comprehensive reviews.^{6,7}

While most of the work done on carbon clusters has focused on neutral species, there is considerable interest in anionic clusters as well. Photoelectron spectroscopy of mass-selected carbon cluster anions has been used to probe the structural evolution of carbon clusters with size.^{8–11} These experiments and higher resolution zero electron kinetic energy (ZEKE) studies¹² also yield electron affinities, vibrational frequencies, and electronic state term values of neutral clusters as well as details about geometry changes that occur upon photodetachment. Further insight into the structural evolution of carbon clusters may also be obtained from ion mobility measurements,¹³ which can only be performed on charged species.

Photodetachment and ion mobility experiments on carbon cluster anions have been complemented by studies of their electronic spectroscopy. The electronic spectra of several of these species have been measured by absorption spec-

troscopy in cryogenic matrices^{2,14–16} and by resonant multiphoton detachment (RMPD) in the gas phase.^{17–21} Maier and co-workers^{22,23} have been particularly active in this area; their results on the gas-phase electronic spectroscopy of C_7^- and anions of similar size suggest that these species—rather than the neutral clusters—may be responsible for the DIB's.²⁴ The experimental spectra coupled with a series of electronic structure calculations^{25–28} have led to a reasonable understanding of the electronic spectroscopy of carbon cluster anions. Thus, for example, the strong optical transition seen for several C_{2n}^- anions has been assigned to the $\tilde{C}^2\Pi_{g(u)} \leftarrow \tilde{X}^2\Pi_{u(g)}$ transition, and two electronic states have been turned to lie below the \tilde{C} state, namely the $\tilde{A}^2\Sigma_{g(u)}^+$ and $\tilde{B}^2\Sigma_{u(g)}^+$ states, where the g and u symmetry labeling alternates with n . For C_6^- , which has a $\tilde{X}^2\Pi_u$ ground state, the experimental term values for the $\tilde{A}^2\Sigma_g^+$ and $\tilde{C}^2\Pi_g$ states are 1.160¹⁶ and 2.042 eV,¹⁸ respectively, while the most recently calculated term value for the optically inaccessible $\tilde{B}^2\Sigma_u^+$ state is 1.32 eV.²⁸

This paper focuses on a less well-understood aspect of carbon cluster anions, namely their relaxation dynamics following electronic excitation. These dynamics are followed using femtosecond photoelectron spectroscopy (FPES).²⁹ In FPES experiments, the species of interest is prepared in an excited state with a broad-bandwidth, ultrafast pump pulse, allowed to evolve for a period of time, and then photoionized or photodetached with an ultrafast probe pulse. By measuring the resulting photoelectron spectrum as a function of pump-probe delay, one obtains a series of “snapshots” of the dynamics induced by the pump pulse. This technique has been used to follow a wide range of chemically significant processes in our laboratory and others but has been applied most frequently to the study of isolated neutral molecules undergoing nonadiabatic electronic relaxation.^{30–37}

^{a)}Present address: Institut für Experimentalphysik, Amimallee 14, Freie Universität Berlin, D-14195 Berlin, Germany.

The application of FPES to carbon cluster anions is motivated by previous experiments conducted by our group on the spectroscopy and electron detachment dynamics of C_4^- , C_6^- , and C_8^- via RMPD with nanosecond lasers.^{17,18} These studies of the $\tilde{C} \leftarrow \tilde{X}$ transitions yielded rotationally resolved features for C_4^- and vibrationally resolved spectra for the other two species. Our experiments also revealed two unusual features concerning the electron detachment dynamics. First, for some transitions, delayed electron ejection was observed over time scales extending up to several hundreds of nanoseconds. In addition, the photoelectron spectra collected following resonant multiphoton excitation were structureless, peaking at low electron kinetic energies (eKE) and decreasing in intensity monotonically toward higher eKE; these PE spectra are in sharp contrast to the structured one-photon PE spectra of these anions.¹⁰ The delayed emission and nature of the multiphoton PE spectra were interpreted as signatures of the cluster analog to thermionic emission, resulting from ground-state clusters with sufficient vibrational energy to eject an electron. We proposed that these highly vibrationally excited clusters were populated from multiple electronic excitation/internal conversion cycles. This mechanism implies that internal conversion following absorption of a single photon occurs faster than 20 ns, the width of the laser pulse used in those experiments.

The FPES experiments described here were undertaken to provide a detailed, explicitly time-domain probe of these dynamics. Specifically, we have applied FPES to C_6^- through excitation of the vibrational origin of the $\tilde{C}^2\Pi_g \leftarrow \tilde{X}^2\Pi_u$ band. The FPE spectra reveal that the subsequent dynamics occurs on two time scales: PE spectral features associated with the initially excited $\tilde{C}^2\Pi_g$ state decay with a lifetime of 730 fs, while intermediate features grow on this same timescale and relax to a final set of states with a time constant of 3.0 ps. We interpret the initial fast dynamics as IC of the $\tilde{C}^2\Pi_g$ state to the intermediate \tilde{B} and possibly \tilde{A} states. Relaxation of the intermediate electronic states to vibrationally hot ground state is complete within ~ 12 ps. The FPE spectra at short times also show strong evidence for a two-electron photodetachment transition, an unusual result that is most likely a reflection of fairly strong configuration interaction between the electronic states of C_6^- .

II. EXPERIMENT

A detailed description of our experimental setup has been described previously.³⁸ Only a brief description will be given here with emphasis on the features specific to the experiment presented in this paper.

Carbon cluster anions were generated from a C_2H_2/CO_2 mixture (2%/2%) in Ar expanded supersonically into vacuum through a combined pulsed valve/discharge assembly³⁹ operating at a repetition rate of 500 Hz. Carbon cluster anions formed in this source discharge were extracted orthogonally into a Wiley–McLaren time-of-flight mass spectrometer.⁴⁰ Laser timing was set such that the mass-selected carbon clusters interacted with the ultrafast excitation and detachment laser pulses at the focus of a “magnetic bottle” time-of-flight

analyzer.⁴¹ The detached electrons were collected with the magnetic bottle at an efficiency of $>50\%$.

The pump and probe pulse were generated from the 790 nm (1.57 eV) fundamental of a regeneratively amplified Ti:sapphire oscillator (Clark MXR) running at 500 Hz in conjunction with various wavelength conversion schemes. The 790 nm pulse, which typically has a 1 mJ pulse energy and a temporal width of 100 fs FWHM (sech^2), was split to pump both an optical parametric generator/amplifier (TOPAS, Light Conversion) and a frequency-tripling unit. Doubled OPA signal served as the excitation pulse for the $\tilde{C}^2\Pi_g \leftarrow \tilde{X}^2\Pi_u$ 0_0^0 transition of C_6^- at 607 nm (2.04 eV, 15 $\mu\text{J}/\text{pulse}$, 100 fs), while tripled fundamental at 263 nm (4.71 eV, 20 $\mu\text{J}/\text{pulse}$, 110 fs) was used as the UV detachment probe. The resulting power density in the interaction region is $\sim 10^{11}$ W/cm², indicating that our experiments are within the weak-field limit. The delay between the pump and probe pulses was set using a computer-controlled translation stage, and the two pulses were collinearly recombined prior to entering the vacuum chamber. The pump and probe pulses were characterized temporally and the absolute zero-of-time within the interaction region determined using two-color above-threshold detachment (ATD)⁴² of I^- .

The electron energy resolution of the spectrometer is limited by the speed of the parent anions at the laser interaction region owing to the large steradiancy collection of the magnetic bottle analyzer.⁴¹ With a parent ion kinetic energy of ~ 1250 eV, the eKE resolution of C_6^- photoelectrons is about 250 meV at an energy of 1 eV and degrades as $(\text{eKE})^{1/2}$. For C_6^- , the TOF spectra were calibrated linearly with respect to kinetic energy by photodetachment of I^- with a 263 nm photon to the two spin-orbit states of iodine. Normalization of the FPE spectra at different delay times was accomplished by alternating scans between the desired delay and a fixed, positive reference delay (2 ps).

III. RESULTS

The one-color PE spectrum of C_6^- taken with the 263 nm probe pulse is shown as dashed curves in Figs. 1(a) and 1(b). The main feature, a peak centered near 0.6 eV, is comprised of transitions from ground state ($\tilde{X}^2\Pi_u$) C_6^- to the $\tilde{X}^3\Sigma_g^-$ ground and $\tilde{a}^1\Delta_g$ first excited electronic states of neutral linear C_6 .¹⁰ These features are not resolved here due to the limited resolution of the magnetic bottle analyzer. A weak but broad feature extending to ~ 5.4 eV arises from two-photon UV detachment of the anion.

The solid curves in Figs. 1(a) and 1(b) are “pump–probe” FPE spectra taken with delays of 200 fs and 12 ps, respectively, between the 607 nm pump and the 263 nm probe pulses. The FPE spectrum in Fig. 1(a) shows new features for $\text{eKE} > 0.75$ eV, and a slight depletion of signal at 0.5–0.6 eV, the peak of the “probe-only” spectrum. Note that the pump–probe spectrum extends to an eKE of ~ 2.5 eV, which corresponds to the maximum allowable kinetic energy, eKE_{max} , given by

$$\text{eKE}_{\text{max}} = h\nu_{pu} + h\nu_{pr} - EA(C_6) = 2.57 \text{ eV}, \quad (1)$$

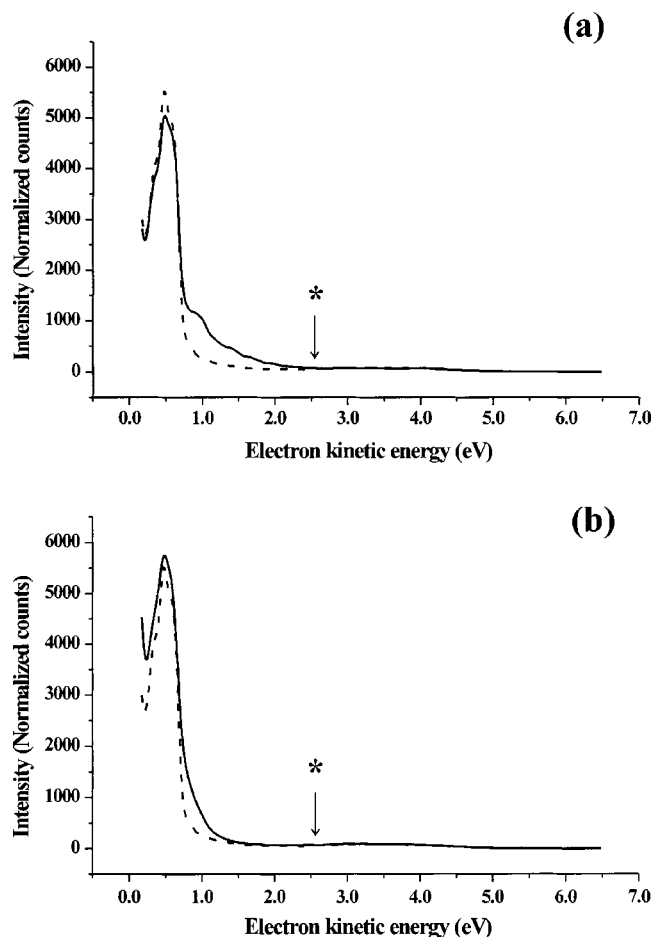


FIG. 1. Comparison of a probe-only photoelectron spectrum (dashed line) with pump-probe spectra (solid lines) at delays of 200 fs (a) and 12 ps (b). Pump and probe wavelengths are 607 and 263 nm, respectively. * shows maximum possible eKE (2.57 eV) from absorption of one-pump and one-probe photon.

using $EA(C_6^-) = 4.180 \text{ eV}$.⁴³ The FPE spectrum in Fig. 1(b) is more similar to the probe-only spectrum, the main difference being that the FPE spectrum extends to somewhat higher eKE.

Figure 2 shows a series of FPE spectra at selected pump-probe delays, Δt , in which a suitably normalized “probe-only” spectrum has been subtracted from the pump-probe spectra. The background-subtracted spectra show the time dependence of the FPE signal more clearly, although the substantial probe-only signal between 0.5 and 0.6 eV makes the background-subtracted intensity less reliable in this region than at higher eKE.

The FPE spectrum measured at 0 fs [Fig. 2(a)] consists of two partially resolved features at 780 meV and 980 meV, and a higher energy “tail” extending to eKE_{max} . This time delay falls within the cross-correlation of the laser pulses and represents the earliest delay at which reasonable background-subtracted signal is observed. At longer times [Figs. 2(b)–2(e)], the high-energy tail decreases in intensity while the lower energy features at 780 and 980 meV grow, reaching a maximum intensity near 1400 fs. While the positions of these lower energy features remain constant up to ~ 1400 fs, they eventually shift to even lower eKE, and by 12 ps they have

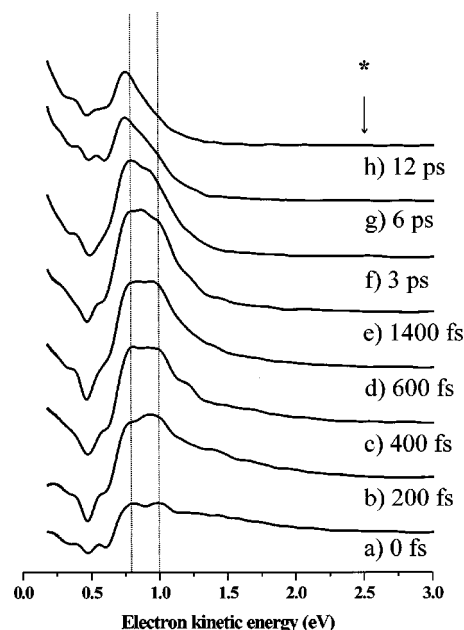


FIG. 2. (a)–(h) Background-subtracted time-resolved photoelectron spectra of C_6^- excited at the origin of the $\tilde{C}^2\Pi_g \leftarrow \tilde{X}^2\Pi_u$ band (607 nm) and probed at various pump-probe delays out to 12 ps. * shows maximum possible eKE. The dashed lines indicate the positions of the two intermediate peaks mentioned in the text.

coalesced into a single peak at 730 meV [Figs. 2(f)–2(h)]. In addition to these trends, the “dip” in the background-subtracted spectra around 0.5 eV fills in with increasing pump-probe delay. Overall, the FPE spectra show evidence for dynamics on at least two time scales: the decay of the high-energy tail and growth of the lower eKE peaks at early times, followed by the evolution of these peaks toward even lower energy at later times.

IV. ANALYSIS

A. Spectral assignments

In order to interpret the FPE spectra, we must correlate the features in the spectra to transitions between anion and neutral electronic states. This requires knowledge of the electronic spectroscopy of C_6^- and C_6 , from which one can extract the energies of the various photodetachment transitions between the two manifolds of electronic states.

The molecular orbital configuration of the C_6^- ground electronic state ($\tilde{X}^2\Pi_u$) is $\dots 6\sigma_g^2 1\pi_u^4 6\sigma_u^2 7\sigma_g^2 1\pi_g^4 2\pi_u^3$. The $\tilde{A}^2\Sigma_g^+$, $\tilde{B}^2\Sigma_u^+$, and $\tilde{C}^2\Pi_g$ states have molecular orbital configurations corresponding to $2\pi_u \leftarrow 7\sigma_g$, $2\pi_u \leftarrow 6\sigma_u$, and $2\pi_u \leftarrow 1\pi_g$ one-electron excitations from the ground state, respectively. The electronic term values for these excited states have been determined through calculations^{26,28} and spectroscopy experiments^{16,18} and are shown in the lower part of Fig. 3.

The electron configuration of the C_6 ground state ($\tilde{X}^3\Sigma_g^-$) is $\dots 6\sigma_g^2 1\pi_u^4 6\sigma_u^2 7\sigma_g^2 1\pi_g^4 2\pi_u^2$. Forney *et al.*¹⁴ located the $^3\Sigma_u^- \leftarrow \tilde{X}^3\Sigma_g^-$ transition at 2.43 eV by matrix absorption spectroscopy. Xu *et al.*¹⁰ mapped out several of the lower-lying electronic states of C_6 by photoelectron spectroscopy.

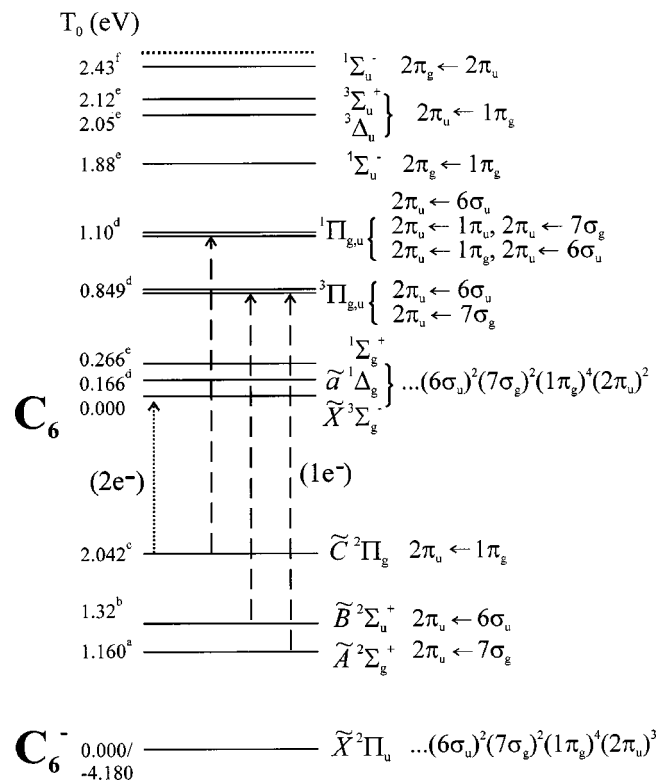


FIG. 3. Term values and dominant electron configurations for C_6^- and C_6 , respectively. Anion term values were obtained from (a) Ref. 16, (b) Ref. 28, and (c) Ref. 18, neutral term values from (d) Ref. 10, (e) Ref. 44, and (f) Ref. 14. $EA(C_6) = 4.180$ eV from Ref. 43. The dashed line 2.57 eV above the neutral ground state indicates the experimental energetic limit. Dashed arrows represent the lowest-energy one-electron photodetachment transitions from each of the low-lying anion excited states. The dotted arrow represents a two-electron photodetachment transition from the \tilde{C} state to the neutral ground state.

copy of C_6^- and assigned them by comparison of the experimentally determined energetics with previous electronic structure calculations; term values of 0.166, 0.849, and 1.10 eV were reported for the $1^3\Pi_u$, $1^3\Sigma_u^+$, and $1^3\Pi_u$ states, respectively. Multireference configuration interaction calculations carried out by Hanrath *et al.*⁴⁴ yield a different energy ordering, with term values of 1.08 and 1.10 eV for the nearly degenerate $1^3\Pi_{u,g}$ states, term values relative to the $\tilde{a}^1\Delta_g$ state of 1.39 and 1.42 eV for the nearly degenerate $1^1\Pi_{u,g}$ states, and a considerably higher term value of 2.12 eV for the $1^3\Sigma_u^+$ state. Since these more recent calculations are of higher quality than those used by Xu *et al.* to assign their spectrum, it is reasonable to revise Xu's assignment by assuming that the energy ordering calculated by Hanrath *et al.* is correct, yielding the neutral energy-level scheme presented in the upper half of Fig. 3. The electronic transitions by which the excited states are accessed from the C_6 ground state, are also shown.

From Fig. 3, one can determine which neutral states are accessible from the various anion states by one-electron photodetachment transitions, which are the transitions that typically dominate a photoelectron spectrum. All neutral states shown in Fig. 3, save the $1^1\Pi_u$ and the $1^1\Sigma_u^-$ states, are accessible from the anion ground state. In contrast, the $\tilde{X}^3\Sigma_g^-$ neutral ground state is not accessible by a one-

TABLE I. eKE_{0-0} values arising from the detachment of various C_6^- electronic states (top) with a 263 nm (4.71 eV) light source through one-electron photodetachment transitions to low-lying C_6 electronic states (left). eKE_{0-0} values were calculated using Eq. (2) from the text and the energetics of Fig. 3.

	$\tilde{C}^2\Pi_g$	$\tilde{B}^2\Sigma_u^+$	$\tilde{A}^2\Sigma_g^+$	$\tilde{X}^2\Pi_u$
$\tilde{X}^3\Sigma_g^-$				0.53
$\tilde{a}^1\Delta_g$				0.36
$1^1\Sigma_g^+$				0.26
$1^3\Pi_{g,u}$		1.00	0.84	
$1^1\Pi_{g,u}$	1.47	0.75	0.59	
$1^1\Sigma_u^-$				
$1^3\Delta_u$	0.52			
$1^3\Sigma_u^+$	0.45			
$2^1\Sigma_u^-$				

electron transition from any of the three excited states of the anion shown in Fig. 3, all of which have a $\dots(2\pi_u)^4$ molecular orbital configuration. The $1^3\Pi_{u,g}$ and $1^1\Pi_{u,g}$ states are the lowest accessible states from the anion $\tilde{A}^2\Sigma_g^+$ and $\tilde{B}^2\Sigma_u^+$ states by one-electron photodetachment transitions, while the $1^1\Pi_u$ state is the lowest neutral state accessible from the $\tilde{C}^2\Pi_g$ state of C_6^- .

The photoelectron spectrum¹⁰ and electronic absorption spectrum^{14,18} of C_6^- are both dominated by $\Delta\nu=0$ vibrational transitions, indicating that there are relatively small geometry changes among the ground and various excited states of C_6 and C_6^- . One therefore expects that $\Delta\nu=0$ transitions dominate the FPE spectra as well. Consequently, one-electron transitions from each anion state will occur near the vibrational band origin for that transition, for which the electron kinetic energy is given by

$$eKE_{0-0} = h\nu_{\text{probe}} - EA_{C_6^-} + T_{C_6^-}^0 - T_{C_6}^0, \quad (2)$$

in which T_X^0 represents the term value for a given electronic state of species X . Values of eKE_{0-0} determined from the best available experimental and theoretical anion and neutral term values are listed in Table I.

As shown in Table I, $eKE_{0-0} = 1.47$ eV for the $1^1\Pi_u \leftarrow \tilde{C}^2\Pi_g$ photodetachment transition, the lowest one-electron transition allowed from the $\tilde{C}^2\Pi_g$ state. This value falls within the high-energy "tail" seen at early pump-probe delay times in Fig. 2, suggesting that this tail and its rapid decay is associated with the initially excited $\tilde{C}^2\Pi_g$ state. The experimentally observed peaks at 780 and 980 meV seen at early times lie close to the eKE_{0-0} values for transitions originating from the anion $\tilde{A}^2\Sigma_g^+$ and $\tilde{B}^2\Sigma_u^+$ states; the peak at 780 meV may correspond to overlapped $1^3\Pi_u \leftarrow \tilde{A}$ and $1^1\Pi_u \leftarrow \tilde{B}$ detachment, while the peak at 980 meV matches eKE_{0-0} for the $1^3\Pi_g \leftarrow \tilde{B}$ transition. These two peaks grow in intensity until around 1400 fs, during which time the high-energy tail disappears. Our somewhat qualitative analysis thus suggests that the initially excited $\tilde{C}^2\Pi_g$ state decays into the intermediate $\tilde{A}^2\Sigma_g^+$ and/or $\tilde{B}^2\Sigma_u^+$ states. This mechanism is considered more quantitatively in the following section.

No significant evolution of the FPE spectra occurs after 12 ps. The spectrum at 12 ps in Fig. 2 shows a peak at 730 meV, the origin of which can be seen in the nonbackground-subtracted spectrum in Fig. 1(b). The latter is just what one would expect from vibrationally hot C_6^- : Hot bands from vibrationally excited anions would yield signal at higher eKE than the probe-only spectrum of cold C_6^- , resulting in a peak in the background subtracted spectrum. The formation of vibrationally excited anions in their ground electronic state at longer times is also consistent with the reduction in amplitude of the “dip” around 0.5 eV; at earlier times this was attributed to depletion of the “probe-only” PE spectrum by the pump pulse. Thus, it appears reasonable to attribute the evolution of the FPE spectra after 1400 fs to internal conversion from the intermediate $\tilde{A}^2\Sigma_g^+$ and $\tilde{B}^2\Sigma_u^+$ states to the anion $\tilde{X}^2\Pi_u$ ground state. The FPE spectrum at long times thus shows the effect of approximately 2 eV of vibrational energy on the PE spectrum of ground state C_6^- .

One issue regarding the above assignment is that the high-energy tail seen at early times extends well beyond eKE_{0-0} for the $1^1\Pi_u \leftarrow \tilde{C}^2\Pi_g$ transition. Even accounting for the significant spectral broadening in our spectrometer, there should be no signal for this transition beyond 1.65 eV, whereas we observe signal out to ~ 2.5 eV, the energetic limit for detachment from the $\tilde{C}^2\Pi_g$ state to the $\tilde{X}^3\Sigma_g^-$ state of C_6 . However, this transition is not one-electron allowed, nor are any transitions to excited C_6 states lying below the $1^1\Pi_u$ state. Hence, one must consider the origin of what appears to be a two-electron transition to the C_6 ground state.

Such a transition could arise from configuration interaction mixing of the $\tilde{C}^2\Pi_g$ state with other C_6^- states of the same symmetry, so long as the C_6 ground state can be accessed via one-electron detachment from these other states. UHF/FOCO/CC calculations by Adamowicz²⁵ have indicated there are two additional C_6^- excited doublet states of Π_g symmetry, the (2) and (3) $^2\Pi_g$ states, for which the calculated term values of 3.06 and 3.68 eV, respectively, are not too far above his calculated term value of 2.62 eV for the $\tilde{C}^2\Pi_g$ state. These two higher-lying states have been assigned experimentally to electronic absorption features at 2.49 and 2.79 eV, respectively, through matrix isolation studies of C_6^- .¹⁶ Both of these states have a nominal $\dots 6\sigma_g^2 1\pi_u^4 6\sigma_u^2 7\sigma_g^2 1\pi_g^4 2\pi_u^4 \pi_g^1$ electron configuration, from which the ground state of C_6 is accessible by $4\pi_g^{-1}$ detachment, making them reasonable potential participants in the configuration interaction mixing required to explain the most energetic electrons observed in our experiment.

B. Relaxation dynamics

In this section, the dynamics revealed by the FPE spectra are examined more quantitatively. The mechanism proposed in the previous section implies that features in the FPE spectra associated with the $\tilde{C}^2\Pi_g$ state of C_6^- should decay exponentially on a time scale of τ_C , where τ_C is the \tilde{C} state lifetime, while those associated with the $\tilde{A}^2\Sigma_g^+$ and $\tilde{B}^2\Sigma_u^+$ states should grow in with time constant τ_C and decay with time constant τ_{AB} , the latter being the lifetime of the inter-

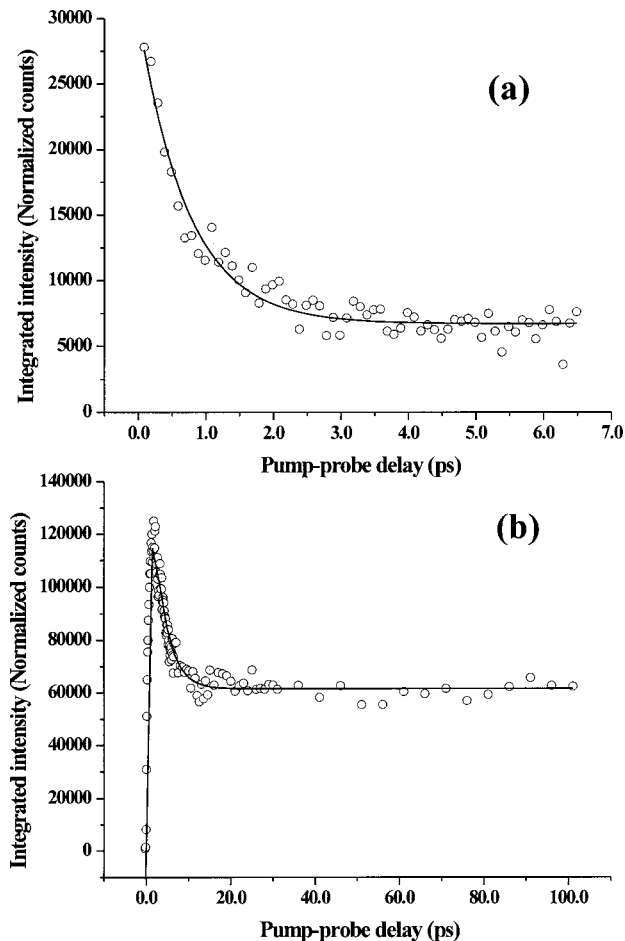


FIG. 4. (a) (Circles) Integrated signal intensity in the 1.45–3.00 eV spectral window, dominated by \tilde{C} state detachment features, plotted with respect to pump–probe delay to 6.5 ps. (Line) Single-exponential fit to integrated intensities [see Eq. (3) in text], $\tau_C = 730 \pm 50$ fs. (b) (Circles) Integrated signal intensity in the 0.63–1.22 eV spectral window, dominated by \tilde{A} and/or \tilde{B} states at short times and the \tilde{X} state at long times, plotted with respect to pump–probe delay to 100 ps. (Line) Exponential association curve fit to integrated intensities [see Eq. (4) in text]: $\tau_C = 730$ fs (fixed); $\tau_{AB} = 3.0 \pm 0.1$ ps.

mediate states with respect to internal conversion to the ground state. This model can be tested as follows.

We have previously associated the high-energy tail in the FPE spectra at early times with the $\tilde{C}^2\Pi_g$ state. In Fig. 4(a), the intensity of this feature integrated from 1.45–3.00 eV, $C(t)$, is plotted versus time and fit to Eq. (3),

$$C(t) = a_1 \exp(-t/\tau_C) + a_0, \quad (3)$$

yielding $\tau_C = 730 \pm 50$ fs. As discussed above, the peaks at 780 and 980 meV are assigned to the intermediate \tilde{A} and \tilde{B} states, and their contribution to the spectra, $AB(t)$, is quantitatively assessed by integrating the electron signal from 0.63–1.22 eV. The result is shown in Fig. 4(b), along with the fit to Eq. (4),

$$AB(t) = b_2 \exp(-t/\tau_{AB}) - b_1 \exp(-t/\tau_C) + b_0, \quad (4)$$

where τ_C is fixed at 730 fs and τ_{AB} is found to be 3.0 ± 0.1 ps.

Good fits to both sets of data are obtained using the same value of τ_C , thus supporting our interpretation of the FPE spectra. Moreover, although there is some latitude in setting the two-energy windows, the best-fit decay times are relatively insensitive to small changes in the spectral intervals used in the analysis; this insensitivity was in fact used as the main criterion for defining the windows. Note, however, that the parameters a_0 and b_0 are nonzero; these represent the “asymptotic” contribution to the signal after the exponential dynamics have finished. (These values reflect the overlap between photoelectron spectra from various anion electronic states, so that photodetachment from more than one state contributes to each of the two energy integration windows shown in Fig. 4). This is particularly true in Fig. 4(b), because the signal from vibrationally hot C_6^- at long delay times (see Fig. 2) contributes significantly to the lower-energy window.

V. DISCUSSION

Our analysis of the FPE spectra of C_6^- indicates that the electronic relaxation from the ground vibrational level of the $\tilde{C}^2\Pi_g$ state occurs in two steps. The initially populated \tilde{C} state decays with a 730 fs lifetime to the \tilde{B} and possibly \tilde{A} states, which collectively give rise to an “intermediate” detachment signal, but which relax on a time scale of 3.0 ps to highly vibrationally excited C_6^- in its ground electronic state. The significance of these time scales, particularly the \tilde{C} state lifetime, can best be appreciated by comparing the time-domain results with the frequency-domain spectrum of C_6^- , and by comparing the relaxation times in C_6^- to those for excited states in comparably sized neutral molecules.

The $\tilde{C} \leftarrow \tilde{X}$ 0_0^0 transition in C_6^- shows no rotational structure and an overall linewidth of 18–20 cm^{-1} ; this is significantly less than the fs pump laser linewidth of 150 cm^{-1} . The measured $\tilde{C}^2\Pi_g$ lifetime of 730 fs corresponds to a spectral linewidth of $\sim 10 \text{ cm}^{-1}$. Since we are clearly not accessing a repulsive potential-energy surface, this linewidth represents the energy spread of the highly excited vibrational levels associated with lower-lying electronic states that are mixed with the zero-order $\tilde{C}^2\Pi_g$ ($v=0$) state and participate in its relaxation dynamics. This 10 cm^{-1} linewidth is substantially larger than the spacing between adjacent rotational levels of the \tilde{C} state, for which $B_e = 0.046 \text{ cm}^{-1}$,²⁶ so the absence of resolved rotational structure in the C_6^- electronic absorption spectrum¹⁸ reflects fundamental dynamics rather than experimental effects resulting from ion temperature, laser bandwidth, saturation effects, etc. We note that preliminary FPE spectroscopy of the $\tilde{C}^2\Pi_u$ state in C_4^- indicates that the initially excited state has a lifetime of >10 ps, consistent with the observation of rotational structure in the $C_4^- \tilde{C} \leftarrow \tilde{X}$ band. In C_6^- , the overall width of the 0_0^0 band of 18–20 cm^{-1} is presumably a convolution of rotational transitions with the 10 cm^{-1} linewidth from lifetime broadening; for comparison, the rotationally resolved 0_0^0 band of C_4^- covers about 15 cm^{-1} with feature widths of 0.1 cm^{-1} .¹⁷

In C_6^- , the second, rather than first, optically accessible electronic state is excited, and it is therefore useful to com-

pare the dynamics seen in our experiment to those observed previously upon excitation of S_2 and higher states in other (neutral) molecules. FPES studies of hexatriene,³⁰ decatetraene,³⁶ phenol,³² and pyrazine³⁵ have shown that $S_2 \rightarrow S_1$ relaxation is the first step in the dynamics, analogous to what is seen for C_6^- , whereas in benzene, $S_2 \rightarrow S_0$ relaxation is reported to be the dominant pathway.³¹ In these earlier FPE studies, the final neutral S_0 state cannot be detected because one-photon ionization of this state was not energetically possible at the photon energies used; the extensive vibrational energy present in the S_0 state is not sufficient to overcome the propensity for vibrational energy to be conserved upon ionization. In our experiment, on the other hand, the dynamics can be followed to completion, since the electron affinity of C_6 is low enough to permit detachment from its ground and excited electronic states at our probe-laser energy.

In pyrazine and the smaller polyenes, the S_2 state lifetime is extremely short, i.e., 50 fs or less,^{30,35,45} and this has been attributed to conical intersections with lower-lying electronic states.⁴⁶ The much longer lifetime of the $C_6^- \tilde{C}^2\Pi_g$ ($v=0$) state suggests that conical intersections do not play a major role in the dynamics. Moreover, the calculated equilibrium geometries of the \tilde{X} , \tilde{A} , \tilde{B} , and \tilde{C} states are quite similar,²⁶ so one would not expect any of the lower-lying states to cross the \tilde{C} state near its minimum where the $v=0$ level is localized.

The situation for C_6^- is probably more akin to that of the S_2 state of decatetraene, the lifetime of which is several hundred femtoseconds.³⁶ In both cases, the relevant electronic absorption spectrum is highly structured,^{14,18,47} and the $v=0$ level of the excited state is embedded in a dense manifold of isoenergetic vibrational levels associated with lower electronic states. We can apply the Beyer–Swinehart state counting algorithm to the $\tilde{B}^2\Sigma_u^+$ and $\tilde{A}^2\Sigma_g^+$ states of C_6^- using calculated²⁶ and experimental^{14,18} vibrational frequencies, when available, and assuming the calculated frequencies for the \tilde{X} state otherwise (i.e., for the bend and antisymmetric stretch modes²⁸). This procedure yields vibrational state densities of 1.08×10^4 and $4.84 \times 10^4 \text{ states/cm}^{-1}$ for the \tilde{B} and \tilde{A} states, respectively, at the energy of the $\tilde{C}^2\Pi_g$ ($v=0$) state, so there is essentially a quasi-continuum of excited state levels with which this state can interact. Given the electronic symmetries of the states involved, the $v=0$ level of the \tilde{C} state will be vibronically coupled to vibrational levels of the \tilde{B} and \tilde{A} states with π_u and π_g symmetry, respectively. Since the doubly degenerate π_u and π_g bending modes are the lowest frequency vibrations, vibrational states with the required symmetry will comprise a significant fraction of the total vibrational state densities. Although the vibrational state density associated with the C_6^- ground state is even higher ($\sim 10^8 \text{ cm}^{-1}$), direct relaxation from the $\tilde{C}^2\Pi_g$ ($v=0$) state to the \tilde{X} states involves much larger changes in vibrational quantum number and is therefore disfavored.

The results presented here are consistent with the multiple absorption/internal conversion model proposed to explain the observation of thermionic emission from C_6^- reso-

nantly excited with ns laser pulses.¹⁸ The time scale for internal conversion to the C_6^- ground state of 3.0 ps is much shorter than the 20 ns pulses used in the previous work, so there is certainly enough time for the ions to undergo several absorption/IC cycles during a 20 ns laser pulse; only 2–3 cycles are required before the anion vibrational energy exceeds the detachment threshold.

VI. CONCLUSIONS

We have used femtosecond photoelectron spectroscopy to investigate the electronic relaxation dynamics of C_6^- following excitation of the $\tilde{C}^2\Pi_g \leftarrow \tilde{X}^2\Pi_u$ band origin. Over a time interval of several picoseconds, the FPE spectra evolve from a spectrum associated with the initially excited $\tilde{C}^2\Pi_g$ state to one associated with highly vibrationally excited C_6^- in its ground electronic state. A more detailed analysis of the FPE spectra shows evidence for two-step relaxation dynamics: internal conversion of the $\tilde{C}^2\Pi_g$ state to the lower-lying $\tilde{B}^2\Sigma_u^+$ and $\tilde{A}^2\Sigma_g^+$ states with a time constant of 730 ± 50 fs, and internal conversion of these intermediate states to the $\tilde{X}^2\Pi_u$ ground state in 3.0 ± 0.1 ps. None of the C_6^- excited states can access the neutral $\tilde{X}^3\Sigma_g^-$ ground state by a one-electron photodetachment transition, and the FPE spectra from the anion excited states are interpreted in terms of photodetachment to low-lying neutral excited states. However, at short times, we observe evidence for a two-electron transition from the $\tilde{C}^2\Pi_g$ anion state to the neutral $\tilde{X}^3\Sigma_g^-$ state and attribute this process to configuration interaction mixing with higher-lying excited states of the same symmetry.

The experiment described in this paper is quite general in that it can be applied to any negative ion with an electronically excited state below the detachment continuum, or, as demonstrated by Gantefor,⁴⁸ to autodetaching electronic states above the detachment threshold. We have obtained preliminary results on C_4^- and C_8^- which, combined with the results presented here, show increasingly rapid relaxation from the \tilde{C} state as the number of carbon atoms increases. Experiments on comparably sized odd carbon cluster anions are also of considerable interest, because while the odd anions have $^2\Pi \leftarrow ^2\Pi$ electronic transitions in the same energy range as the even clusters, there are no intermediate $^2\Sigma$ electronic states in the odd clusters and, therefore, the dynamics might be expected to be qualitatively different.⁴⁹

ACKNOWLEDGMENTS

This research is supported by the National Science Foundation under Grant No. DMR-9814677. One of the authors (A.E.B.) is an NSF predoctoral fellow. The author C.F. gratefully acknowledges postdoctoral support from the Deutsche Akademie der Naturforscher Leopoldina (Grant No. BMBF-LPD 9801-6). The author R.W. acknowledges support from the Feodor Lynen Programm of the Humboldt Foundation.

- ¹A. E. Douglas, *Nature (London)* **269**, 130 (1977).
- ²J. Fulara, D. Lessen, P. Freivogel, and J. P. Maier, *Nature (London)* **366**, 439 (1993).
- ³H. W. Kroto and K. McKay, *Nature (London)* **331**, 328 (1988).
- ⁴H. W. Kroto, J. R. Heath, S. C. O'Brien, R. F. Curl, and R. E. Smalley, *Nature (London)* **318**, 162 (1985).
- ⁵S. Ijima, *Nature (London)* **354**, 56 (1991).
- ⁶W. Weltner and R. J. Van Zee, *Chem. Rev.* **89**, 1713 (1989).
- ⁷A. Van Orden and R. J. Saykally, *Chem. Rev.* **98**, 2313 (1998).
- ⁸S. Yang, K. J. Taylor, M. J. Craycraft, J. Conceicao, C. L. Pettiette, O. Cheshnovsky, and R. E. Smalley, *Chem. Phys. Lett.* **144**, 431 (1988).
- ⁹D. W. Arnold, S. E. Bradforth, T. N. Kitsopoulos, and D. M. Neumark, *J. Chem. Phys.* **95**, 8753 (1991).
- ¹⁰C. Xu, G. R. Burton, T. R. Taylor, and D. M. Neumark, *J. Chem. Phys.* **107**, 3428 (1997).
- ¹¹H. Handschuh, G. Gantefor, B. Kessler, P. S. Bechthold, and W. Eberhardt, *Phys. Rev. Lett.* **74**, 1095 (1995).
- ¹²C. C. Arnold, Y. X. Zhao, T. N. Kitsopoulos, and D. M. Neumark, *J. Chem. Phys.* **97**, 6121 (1992).
- ¹³N. G. Gotts, G. von Helden, and M. T. Bowers, *Int. J. Mass Spectrom. Ion Processes* **149/150**, 217 (1995).
- ¹⁴D. Forney, J. Fulara, P. Freivogel, M. Jakobi, D. Lessen, and J. P. Maier, *J. Chem. Phys.* **103**, 48 (1995).
- ¹⁵P. Freivogel, J. Fulara, M. Jakobi, D. Forney, and J. P. Maier, *J. Chem. Phys.* **103**, 54 (1995).
- ¹⁶P. Freivogel, M. Grutter, D. Forney, and J. P. Maier, *J. Chem. Phys.* **107**, 22 (1997).
- ¹⁷Y. Zhao, E. de Beer, and D. M. Neumark, *J. Chem. Phys.* **105**, 2575 (1996).
- ¹⁸Y. Zhao, E. de Beer, C. Xu, T. R. Taylor, and D. M. Neumark, *J. Chem. Phys.* **105**, 4905 (1996).
- ¹⁹M. Tulej, D. A. Kirkwood, G. Maccaferri, O. Dopfer, and J. P. Maier, *Chem. Phys.* **228**, 293 (1998).
- ²⁰M. Ohara, H. Shiromaru, Y. Achiba, K. Hashimoto, S. Ikuta, and K. Aoki, *J. Chem. Phys.* **103**, 10393 (1995).
- ²¹M. Ohara, D. Kasuya, H. Shiromaru, and Y. Achiba, *J. Phys. Chem. A* **104**, 8622 (2000).
- ²²J. P. Maier, *Chem. Soc. Rev.* **26**, 21 (1997).
- ²³J. P. Maier, *J. Phys. Chem. A* **102**, 3462 (1998).
- ²⁴M. Tulej, D. A. Kirkwood, and M. Pachkov, *Astrophys. J. Lett.* **506**, L69 (1998).
- ²⁵L. Adamowicz, *Chem. Phys. Lett.* **182**, 45 (1991).
- ²⁶S. Schmatz and P. Botschwina, *Chem. Phys. Lett.* **235**, 5 (1995).
- ²⁷S. Schmatz and P. Botschwina, *Chem. Phys. Lett.* **245**, 136 (1995).
- ²⁸Z. Cao and S. D. Peyerimhoff, *J. Phys. Chem. A* **105**, 627 (2001).
- ²⁹D. M. Neumark, *Annu. Rev. Phys. Chem.* **52**, 255 (2001).
- ³⁰D. R. Cyr and C. C. Hayden, *J. Chem. Phys.* **104**, 771 (1996).
- ³¹W. Radloff, V. Stert, T. Freudenberg, I. V. Hertel, C. Jouvet, C. Dedonder-Lardeux, and D. Solgadi, *Chem. Phys. Lett.* **281**, 20 (1997).
- ³²C. P. Schick, S. D. Carpenter, and P. M. Weber, *J. Phys. Chem. A* **101**, 10470 (1999).
- ³³M. Schmitt, S. Lochbrunner, J. P. Shaffer, J. J. Larsen, M. Z. Zgierski, and A. Stolow, *J. Chem. Phys.* **114**, 1206 (2001).
- ³⁴C. P. Schick and P. M. Weber, *J. Phys. Chem. A* **105**, 3735 (2001).
- ³⁵V. Stert, P. Farmanara, and W. Radloff, *J. Chem. Phys.* **112**, 4460 (2000).
- ³⁶V. Blanchet, M. Z. Zgierski, and A. Stolow, *J. Chem. Phys.* **114**, 1194 (2001).
- ³⁷C. P. Schick and P. M. Weber, *J. Phys. Chem. A* **105**, 3725 (2001).
- ³⁸B. J. Greenblatt, M. T. Zanni, and D. M. Neumark, *Chem. Phys. Lett.* **258**, 523 (1996).
- ³⁹D. L. Osborn, D. J. Leahy, D. R. Cyr, and D. M. Neumark, *J. Chem. Phys.* **104**, 5026 (1996).
- ⁴⁰W. C. Wiley and I. H. McLaren, *Rev. Sci. Instrum.* **26**, 1150 (1955).
- ⁴¹O. Cheshnovsky, S. H. Yang, C. L. Pettiette, M. J. Craycraft, and R. E. Smalley, *Rev. Sci. Instrum.* **58**, 2131 (1987).
- ⁴²M. D. Davidson, B. Broers, H. G. Muller, and H. B. van Linden van den Heuvel, *J. Phys. B* **25**, 3093 (1992).
- ⁴³D. W. Arnold, S. E. Bradforth, T. N. Kitsopoulos, and D. M. Neumark, *J. Chem. Phys.* **95**, 8753 (1991).
- ⁴⁴M. Hanrath, S. D. Peyerimhoff, and F. Grein, *Chem. Phys.* **249**, 121 (1999).
- ⁴⁵X. P. Ci and A. B. Myers, *J. Chem. Phys.* **96**, 6433 (1992).

⁴⁶A. L. Sobolewski, C. Woywod, and W. Domcke, *J. Chem. Phys.* **98**, 5627 (1993).

⁴⁷W. G. Bouwman, A. C. Jones, D. Phillips, P. Thibodeau, C. Friel, and R. L. Christensen, *J. Phys. Chem.* **94**, 7429 (1990).

⁴⁸S. Minemoto, J. Muller, G. Gantefor, H. J. Munzer, J. Boneberg, and P. Leiderer, *Phys. Rev. Lett.* **84**, 3554 (2000).

⁴⁹Z. Cao, S. D. Peyerimhoff, F. Grein, and Q. Zhang, *J. Chem. Phys.* **115**, 2062 (2001).